polymer papers

Molecular modelling of the structure of a wholly aromatic thermotropic copolyester

D. Hofmann*, A. I. Schneider and J. Blackwell†
Department of Macromolecular Science, Case Western Reserve University, Cleveland, OH 44106, USA
(Received 19 November 1993; revised 10 May 1994)

This paper describes the application of molecular mechanics modelling to study the solid-state structure of the thermotropic copolyester prepared from *p*-hydroxybenzoic acid and 2-hydroxy-6-naphthoic acid. X-ray analysis of as-spun fibres shows that the structure consists of parallel, highly extended chains of completely random comonomer sequence which are packed on an orthorhombic pseudo-hexagonal network and ordered in three dimensions. Molecular models for arrays of chains of the 75/25 copolymer were constructed with chain extension and lateral packing as suggested by the X-ray data. Typical starting models consisted of 19 non-identical sequences of 12 monomers in a variety of conformations. The models were optimized by potential energy minimization using the SYBYL® software package. Results for minimization of 20 such arrays, with different sequences and starting conformations, suggest that there are a large number of multiple minima of approximately equal energy. The main effect of the refinement was to change the aromatic ester torsion angles and thus eliminate the bad contacts between adjacent chains. In the final models, the aromatic ester torsion angles are distributed about means that are close to those observed in low molecular weight model compounds. Most importantly, the potential energies of the copolymer arrays are similar to those predicted for analogous models of the two homopolymers, indicating that there are no significant problems in packing non-identical chains of the copolymers on the same lattice. In addition, we have simulated the X-ray diffraction data by calculating the cylindrically averaged scattering intensity transforms for the models of arrays of chains. We find that even the small arrays considered here predict the observed Bragg reflections on the equator and first layer line, as well as the non-periodic meridional maxima, and the results are sensitive enough to allow for selection between different possible conformations.

(Keywords: molecular modelling; thermotropic copolyester; X-ray diffraction)

INTRODUCTION

X-ray diffraction patterns for thermotropic wholly aromatic copolyesters are particularly interesting because they demonstrate the existence of three-dimensional order despite the fact that the chains have random sequence. The most studied polymer in this class is that prepared from *p*-hydroxybenzoic acid (HBA) and 2-hydroxy-6-naphthoic acid (HNA), hereafter referred to as copoly(HBA/HNA), which is the basis of the VECTRA® products of Hoechst–Celanese. A typical X-ray pattern for 75/25 copoly(HBA/HNA) is shown in *Figure 1*. The pattern shows that the chains of the 75/25 copolymer are packed on an orthorhombic (pseudo-hexagonal) network with dimensions $a=9.18$ Å and $b=5.30$ Å[1–4]. The layer lines are non-periodic, and their positions are predicted accurately from the structural correlations along an extended copolymer chain of completely random comonomer sequence. The existence of a Bragg maximum on the first layer line requires the existence of three-dimensional order, i.e. there is registration of the chains along the fibre axis direction. The intensity distribution is consistent with an approximately body-centred structure in which the planes of successive aromatic units along the chain are inclined with respect to each other and adjacent chains are staggered by one monomer. Beyond this, there has been some disagreement over the nature of the three-dimensional order. Windle and coworkers[5,6] have suggested that identical non-repeating sequences aggregate to form 'non-periodic lattices'. They have constructed models of arrays of chains of identical sequences in which the monomers are approximated as points, and have shown that the characteristics of the observed diffraction patterns are generated when the predicted scattering is averaged over a number of arrays (each having a different comonomer sequence). However, it has been the view in this laboratory[1–3] that such a segregation of short identical sequences is unnecessary to explain the X-ray data, which in any case is unlikely to account for the large lateral crystal size and degree of crystallinity. We have shown that we can predict the diffraction characteristics by a much more minimal registration in which short non-identical sequences form layers with their centres approximately on a common plane perpendicular to the chain axis.

* Present address: Gkss-Forschungszentrum, Abteilung für membranforschung, D-14513 Teltow-Seehof, Germany
† To whom correspondence should be addressed

0032-3861/94/26/5603–08

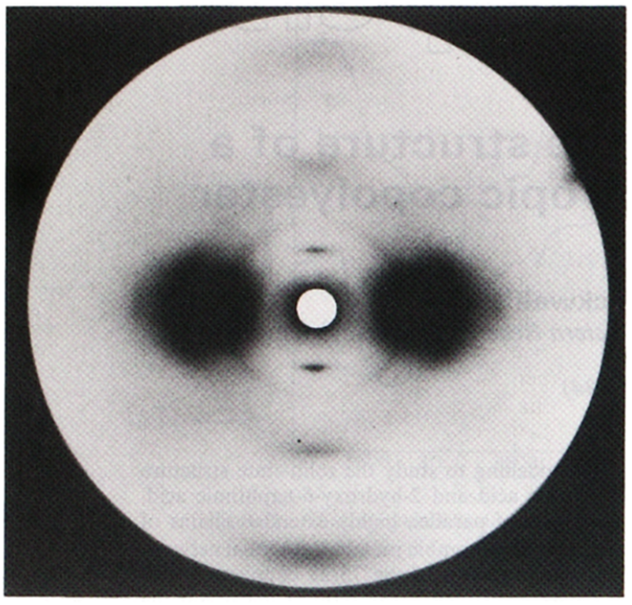

Figure 1 X-ray fibre diagram for as-spun 75/25 copoly(HBA/HNA). The fibre direction is vertical

Simulations of the diffraction data using both of the approaches above require approximations: Windle and coworkers used point monomers and only a finite number of different sequences; the simulations in this laboratory required averaging over all possible sequences before we considered the effects of packing. The central question that needs to be addressed is whether non-identical chains can actually be packed according to the lattice dimensions defined by the X-ray data. We have used molecular mechanics modelling to predict the structures of arrays of non-identical chains of copoly(HBA/HNA). This work follows on from previous molecular modelling studies of the conformation[7], stiffness[8,9] and packing[10–13] of thermotropic polymers. The approach makes it possible to study the intermolecular interaction of actual chains without the approximations and averaging used in previous modelling studies for the X-ray simulations. Although the size of the calculations involved has restricted us to a detailed consideration of a relatively small number of models, we believe that the results go a long way towards solving the remaining structural problems.

In the calculations described below, the models subjected to energy minimization consisted of 19 chains each of 12 monomers with an overall HBA/HNA molar ratio of 75/25. Such a model contains 3363 atoms, and is necessarily considered within the constraints established by the X-ray data for the chain extension and lateral packing[14–18]. Chivers *et al.*[16] showed that the wide angle meridional maxima were consistent with a completely random sequence of HBA and HNA residues in a highly extended chain conformation. Their analyses required axial advances for the HBA and HNA residues that are close to their lengths but nevertheless permit a somewhat sinuous conformation, consistent with the mechanical property data[19]. Strong equatorial maxima at $d=4.55$ Å, 2.63 Å and 2.29 Å can be indexed by a hexagonal lattice with $a=b=5.3$ Å. The strong reflection on the first layer line at $d=3.3$ Å is not on a row containing an equatorial reflection. It is indexed $hk=21$ for a two-chain orthorhombic unit cell with $a=9.18$ Å and $b=5.30$ Å. This structure is analogous to that for the high temperature form of the homopolymer poly(HBA)[4,20,21], in which the c axis repeat of 12.5 Å contains two monomer units with successive aromatic planes mutually inclined by approximately 60° and the monomers on adjacent chains packed in a 'herring-bone' array.

The non-periodic layer lines arise from the structural correlations in chains in which the axial advance may be one of two different distances which are a little less than the lengths of the HBA and HNA residues, i.e. 6.35 Å and 8.37 Å, respectively, measured from ester oxygen to ester oxygen. The observed meridional d spacings vary with monomer ratio, except for that at $d=2.07$ Å[15,22]. This invariant maximum corresponds approximately to the third order of the HBA axial advance and the fourth order of the HNA axial advance, and can be thought of as a Bragg reflection for a partially filled one-dimensional lattice with $c=2.07$ Å. The half-width of this maximum (in the chain axis direction) yields a 'crystallite size' of 70–80 Å depending on the monomer ratio, corresponding to a correlation length for the extended chain conformation of 10–12 monomers. These observations indicate that in constructing models for the ordered regions we need to consider chains of about 12 monomers. Line broadening measured for the equatorial maximum at $d=4.55$ Å yields a crystallite dimension of ~ 70 Å perpendicular to the chain axis, which means that the ordered regions consist of about 200 chains. We have been limited to considering 19 chains in most of our models, owing to computer time and memory limitations, although in some simulations larger models were considered.

EXPERIMENTAL

Atomic coordinates for the HBA and HNA monomer residues were derived using the standard bond lengths and angles contained within the SYBYL® software package (Tripos Associates, St Louis, MO). Models for the chains were constructed as sequences of the four possible dimers. As an example, the HBA/HNA dimer is

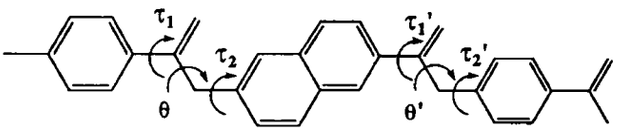

The zero positions for the linkage torsion angles are for the planar conformations; positive angles correspond to clockwise rotations. Model compounds and energy minimization indicate that the ester group is approximately planar ($\theta=180°$) and approximately coplanar with the aromatic group attached to the carbonyl ($\tau_1=0°$ or 180°). In addition, the planes of successive aromatic moieties are inclined at approximately 60° ($\tau_2=\pm 60°$ or $\pm 120°$). The HNA residue was restricted to the shorter *cis* conformation ($\tau_1'=180°$, as shown), as suggested by the mechanical properties[19] and consistent with the axial advance per residue refined from the X-ray analysis.

Within the above definition coonsiderable degeneracy is possible, and it is useful to define a further parameter δ, namely the angle between the axial projections of successive carbonyl vectors. The parameter δ is used to

define two chain conformations: conformation I, analogous to that determined for poly(HBA), which has alternating $\delta = +120°$ and $-120°$; and conformation II, in which the planes of the ester groups are the same as in conformation I but there is random disposition of the C=O vectors, i.e. the ester groups can be flipped by 180° (subject to the limitation that HNA always has the *cis* conformation). As an example, if the mutual orientation of carbonyls on residues 1 and 2 is set at $\delta = 120°$, then δ for residues 2 and 3 can be either $+60°$ or $-120°$.

Axial projections for chains of 12 residues in conformations I and II are shown in *Figure 2*. Conformation I with symmetric dispositions of the carbonyls to one side of the chain can be described as a 'butterfly conformation'. Conformation II with random dispositions of the carbonyls to both sides of the chain can be described as a 'distorted butterfly'.

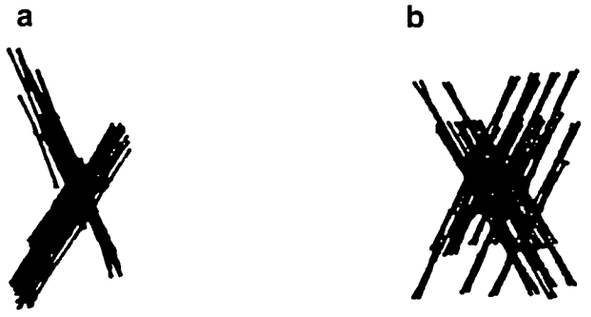

Figure 2 Axial projections of chains of 12 residues: (a) conformation I ('butterfly'); (b) conformation II ('distorted butterfly')

Chains of 12 residues were constructed from the monomer models with random sequences selected using a random number generator subject only to the requirement of an overall HBA/HNA monomer composition in the arrays. Note that the number of HBA and HNA residues was not the same in each of the 12 residue segments, which therefore had different lengths. In constructing an array, all the chains had conformations of the same type (I or II). The z axis of the chain was taken as the best least-squares line through the coordinates. The origin of the xy projection was placed at a node of a hexagonal network with $a = 5.3$ Å. The chains in an array were registered by setting the ester oxygen of the central (seventh) monomer at $z = 0$. The packing of the chains was described by an orthorhombic network with $a = 9.2$ Å and $b = 5.3$ Å, where each cell contained projections of two chains passing through the origin and centre. Adjacent monomers in the register plane were packed in an approximate herring-bone pattern: the projection of the aromatic plane of the first monomer of the chain through the origin was inclined at 60° to the bc plane and was parallel to the plane of the second monomer in the central chain. For conformation I, this condition can be achieved in two ways, as is illustrated in *Figure 3*: either the 'butterflies' are pointing in the same direction along the a axis or are alternating. These two types of packing are designated A and B.

The arrays subjected to energy minimization consisted of 19 non-identical chains of 12 monomers. Sufficient arrays were considered so as to explore the effects of different chain sequences, starting conformations and packing. The copoly(HBA/HNA) chain has a sense, and in principle we also need to consider parallel, antiparallel

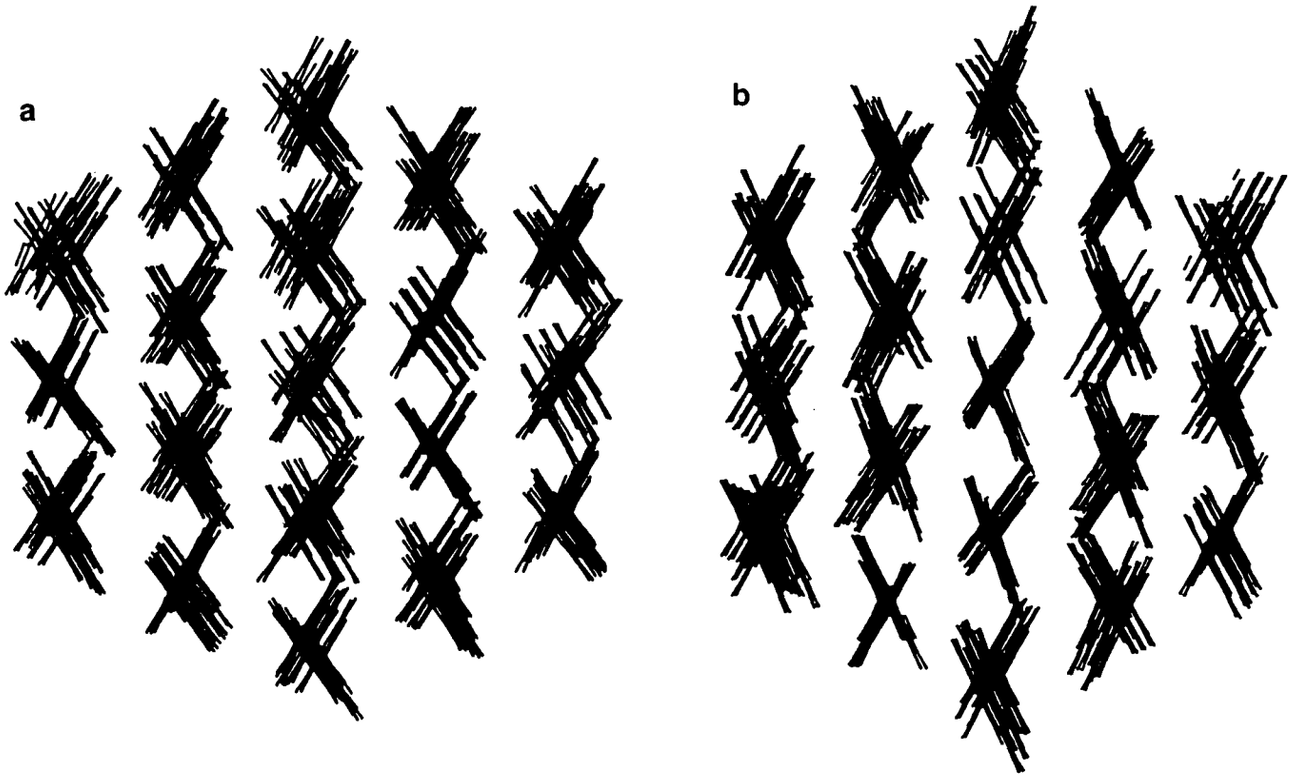

Figure 3 Axial projections of chains of 12 residues of conformation I with (a) parallel (type A) and (b) antiparallel (type B) packing

and random polarity packing. However, we found relatively little sensitivity to chain sense in either the modelling or the X-ray simulations. We have therefore confined the presentation here to results for models in which all the chains have the same sense. Note that the homopolymers are reported to crystallize with the chains having parallel sense[23]. In the quenched copolymers one might expect random polarity or perhaps some preference for parallel polarity in an otherwise random arrangement.

Energy minimization was done using the Tripos SYBYL® package loaded onto a Silicon Graphics 4D/220 computer. The energy was calculated using the Tripos force field as the sum of the bond-stretching, bond angle bending, out-of-plane bending, van der Waals non-bonded interactions and electrostatic energy contributions. The copolymer arrays consisted of 3363 atoms, approaching the limit that could be accommodated by both the software package and the computer memory. Minimization of an array using a three-dimensional periodic boundary condition was not possible because the chains had different lengths. Even in the a and b directions, a periodic boundary condition is inadequate in modelling the present structures where all the chains are different. Minimization of the free-standing array of 19 chains was complete in approximately 48 h. However, there was considerable contraction, in some cases resulting in a density increase of approximately 10%, together with significant deviation from the pseudo-hexagonal packing.

We approached the boundary problem using a three-step procedure. First, the structure of the seven inner chains was optimized while the outer chains remained fixed. Thereafter, the seven central chains were held constant while the energy of the 12 outer chains was minimized. The first step was then repeated, holding the outer chains fixed while the energy of the seven inner chains was minimized. Contraction occurred at the second step, but this was minimal (1–2% in density) and within the experimental error of the determined unit cell dimensions. This whole process was complete in 90 h of processor time. Repeating steps two and three had very little effect on the structure and energy of the array. Consequently, the three-step process was taken as an approximation to a boundary condition. The results presented below are for 20 different arrays optimized in this manner.

X-ray diffraction by the arrays was simulated by calculating the cylindrically averaged intensity transform $I(R,Z)$ via

$$I(R,Z)=\sum_{n=-n'}^{n'}\left|\sum_{j=1}^{N} f_j J_n(2\pi R r_j)\exp(2\pi i Z z_j - n\phi_j)\right|^2$$

where f_j is the atomic scattering factor of the jth of N atoms in the array, with cylindrical polar coordinates r_j, θ_j and z_j; R and Z are the reciprocal space coordinates of the cylindrically averaged Fourier intensity transform $I(R,Z)$; and J_n represents the cylindrical Bessel functions of order up to $n'=10$. This expression was used to calculate the intensity on the equator and on the first layer line at $Z=0.078\ \text{Å}^{-1}$.

The X-ray scattering for the 19 chain arrays was predicted along the meridional direction and along the equator and first layer lines. The arrays are small in the lateral direction, being only five chains wide across the diameter. Consequently, the primary peaks will be much broader than those observed, and there will also be significant subsidiary maxima. In the axial direction, the layer lines may be shifted owing to the fact that we are averaging over only 19 possible sequences.

To probe the sensitivity of the diffraction calculations, we simulated the diffraction patterns for larger arrays of 127 non-identical chains of four monomers, all having their central ester oxygens in a register plane. It will be seen that these slices of the structure were sufficiently thick to generate Bragg maxima on the first layer line, although they were too large for optimization by energy minimization.

RESULTS AND DISCUSSION

Energy minimization

Prior to setting up the models for the chains, we explored the energetics of the conformations of the four individual dimers. The energy minima for all four were close to $\tau_1=0°$ and 180°, $\theta=180°$ and $\tau_2=\pm60°$ and $\pm120°$. *Figure 4a* shows a plot of energy *versus* τ_1 for the HBA/HNA dimer while θ and τ_2 were set at 180° and 60°, respectively; *Figure 4b* shows a similar plot for

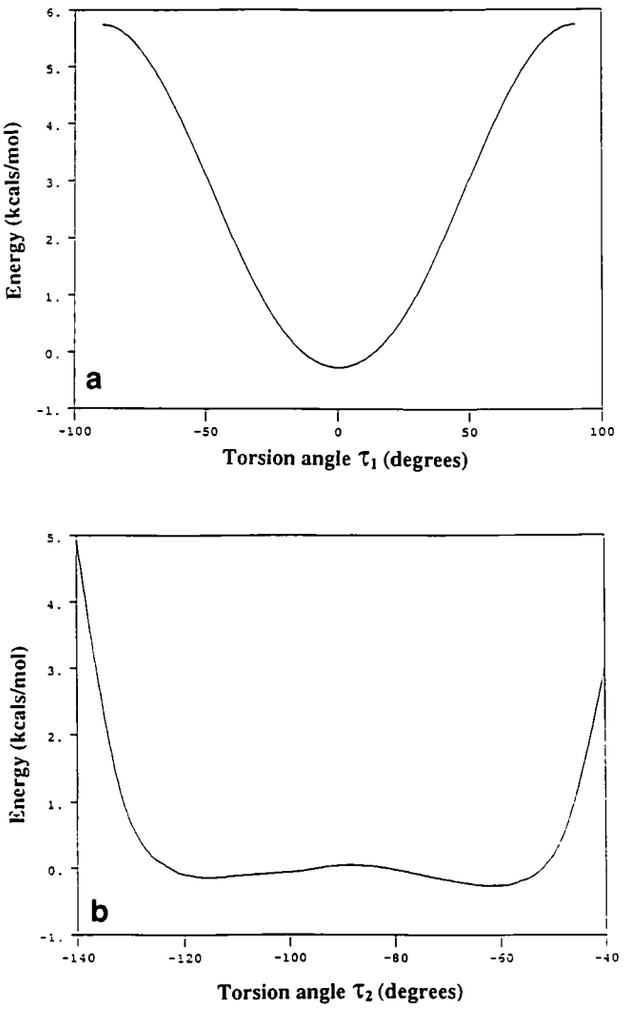

Figure 4 Plots of energy of the HBA/HNA dimer as a function of (a) τ_1 when $\theta=180°$ and $\tau_2=60°$ and (b) τ_2 when $\tau_1=0°$ and $\theta=180°$

variation of τ_2, with τ_1 and θ set at 0° and 180°, respectively. It can be seen that the energy minima are relatively broad, and thus τ_1 and τ_2 can be changed significantly with only a relatively minor effect on the total energy. The minimum energy conformations predicted for the dimers are close to those observed for relevant model compounds[24-31].

Twenty starting models, each of 19 different chains of 12 monomers with an overall 75/25 HBA/HNA monomer ratio, were subjected to energy minimization by the three-step procedure described above. The models were selected so that we could consider mixtures of different sequences, starting conformations (I or II) and packing models (A or B). For all the starting models, the calculated potential energy was very high (in excess of 10^4 kcal; 1 cal = 4.2 J) owing to overlap of monomers on different chains. This is to be expected in view of the non-identical sequences and the regularity of the starting conformations. Minimization of the arrays led to models which had potential energies in the range −1300 kcal to −1450 kcal, with most being closer to the lower figure. (These data are for the three-step minimization described above. It is interesting that the one-step minimization of the arrays led to energies in the same range, although these energies were generally closer to the higher figure (−1300 kcal), probably reflecting the effects of lattice contraction.)

For comparison, we performed the same kind of calculations for the homopolymer poly(HBA) using the same lattice parameters, starting conformations and packing models. After minimization, we obtained models with energies in the range −1200 kcal to −1300 kcal. These figures are actually higher than those obtained for the copolymer models, which probably reflects the different number of atoms (3021 for the homopolymer, 3363 for the 75/25 copolymer). The copolymer structure exists at room temperature; the pseudo-hexagonal structure for the homopolymer exists only at high temperature, and is even more open. For the equivalent poly(HNA) structure (4389 atoms), the energy is a little lower at −1780 kcal. The significant point is that the energies for both homopolymer models are not greatly different from those for the copolymer, and they demonstrate that the random chains of the copolymer can be packed on the observed lattice with relatively little difficulty. It means that there are no packing problems that would serve as the driving force for segregation of identical sequences, which are presumed as the rationale for the sequence segregation model proposed by Windle and coworkers[5,6].

The differences between the starting and final models occur almost entirely in the aromatic ester torsion angles τ_1 and τ_2. Even so, the averages for these angles are close to the energy minima for the isolated dimers. A survey of the ester torsion angles yields the following averages (and standard deviations): $\tau_1 = 0°(10°)$, $|\theta| = 175°(4°)$ and $|\tau_2| = 70°(11°)$. Values of $|\tau_2|$ greater than 90° were converted to $180° - |\tau_2|$ before averaging. Positive and negative values for τ_2 and θ occur with approximately equal frequency. These data are for the seven central chains for the 20 minimized arrays. The outer chains were omitted because of possible distortions from edge effects, although in retrospect the inclusion had almost no effect on the final averages. The conformational changes that occur are seen most easily in *c* axis projections of starting and energy-minimized arrays, as shown in *Figure 5*. The

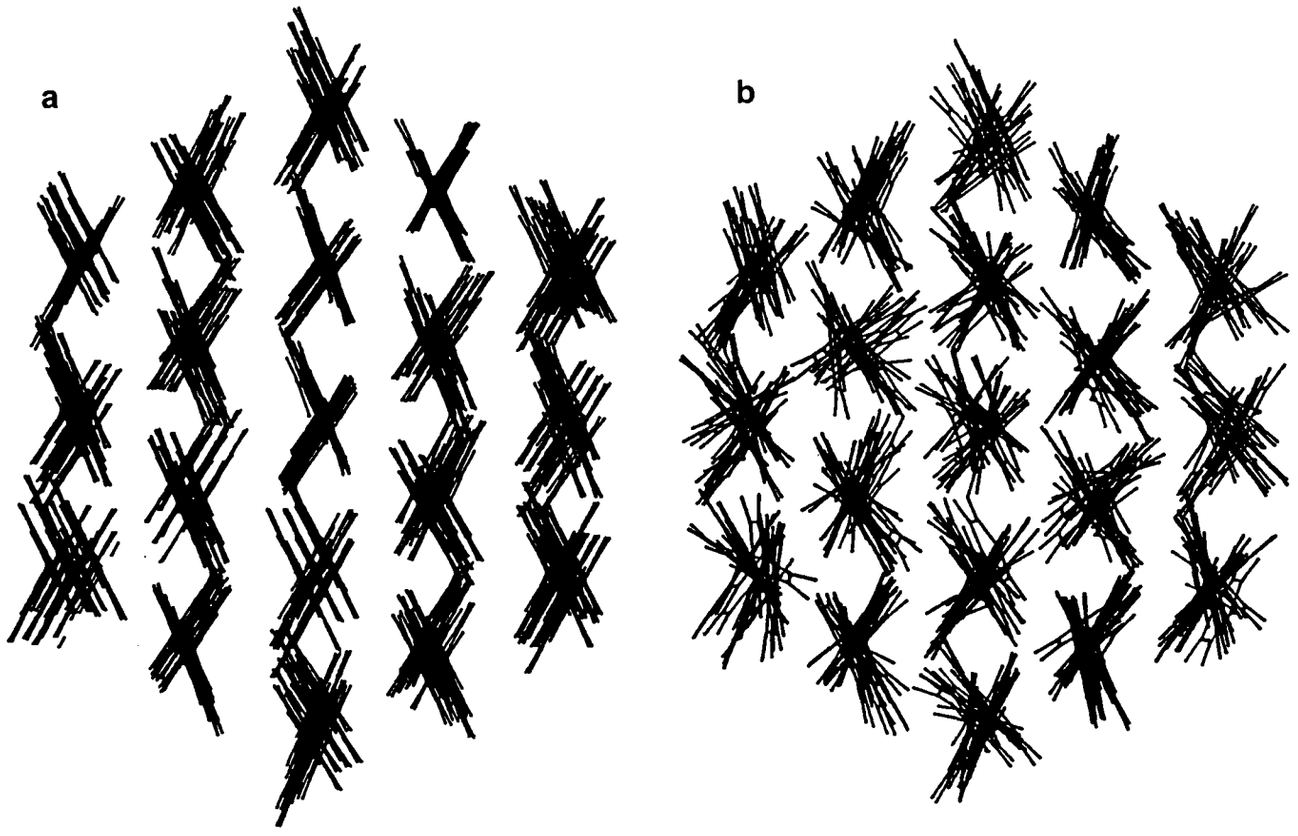

Figure 5 Axial projections of an array of 19 chains of 12 residues with conformation I and type B packing: (a) starting array; (b) energy-minimized array

straight lines are the projections of the aromatic units, which start out inclined alternately by $\pm 60°$ but adjust to a distribution of orientations such that the chain has an almost cylindrical projection. However, this effect is only appreciated in projections involving a number of residues (in this case 12 per chain). The standard deviations indicate that the changes from one residue to the next are relatively small.

The 19 chains of the starting models were arranged in register at their centres such that the central ester oxygen was at $z=0$. The energy minimization resulted in relatively little change in this registration. There were small axial shifts, but the standard deviation about the origin plane was only 0.2 Å. This result is not surprising since even if better local packing was made possible by shifting the chain by one monomer along the z axis, such a shift is unlikely to occur during molecular mechanics modelling given the cooperative conformational changes that would be necesssary to move the chain in a screw-like manner. In addition, in the present model consisting of finite chains of the same number of monomers, end effects would favour approximate registration at the centre so as to avoid exposed monomers at the chain ends. The latter problem could be avoided by limiting the energy minimization to the central region of an array of finite chains. Even so, dynamic modelling would probably be necesssary to simulate chain shifts, which is outside the range of feasible computation on our system.

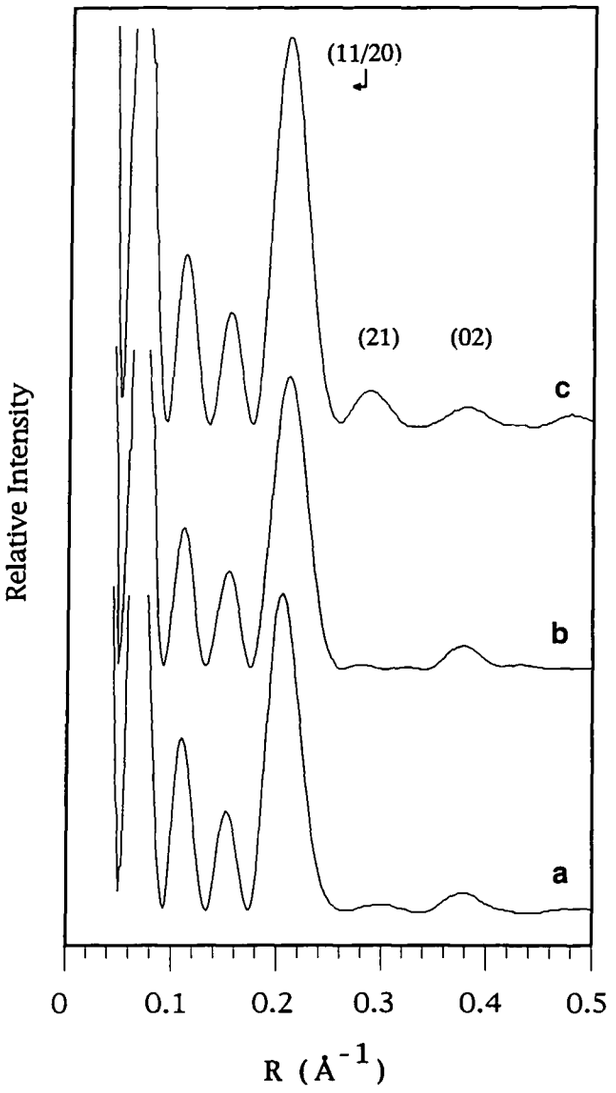

Figure 6 Predicted X-ray scattering on the equator for energy-minimized arrays of 19 chains of 12 residues. The starting models had (a) chains with conformation II, (b) type A packing of chains with conformation I and (c) type B packing of chains with conformation I

It seems likely that the registration of random sequences in the actual polymer occurs at least in part because of the dipole–dipole interactions between the ester groups. However, there was very little difference between models refined with and without inclusion of electrostatic terms. It appears that end effects predominate in these models consisting of relatively short chain segments, although this may not be the case in the polymer where the degree of polymerization is ~ 150. Similarly, the basic features of the chain conformation and packing defined in the starting models are retained after energy minimization. For example, the butterfly characteristics of conformation I in type B packing are still apparent in the projection of the minimized structure shown in *Figure 5b*. Once the δ angles are set, i.e. the mutual orientations of the C=O bonds of adjacent residues, they change only by 10–30°. There are no 180° flips of the ester orientation. One would assume that such flips would improve the packing of certain sequences, but the molecular mechanics minimization is insufficient to achieve them. Again, we would expect that such conformational changes would be predicted in dynamic modelling.

Our approach to the limitations of molecular mechanics has been to refine multiple models. Despite the fact they have different sequences, starting conformations and packing, they all minimize to structures with energies between -1300 kcal and -1450 kcal. Indeed, most of the models considered had energies in the lower half of the range. It would seem unlikely that any of these are global minima, but rather that there are a very large number of almost equivalent minima. For arrays containing $19 \times 12 = 228$ monomers, the energies of most of the minimized models are within 0.3 kcal mol^{-1} monomer. Our view is that these approximately equivalent structures are representative of the many arrangements that occur in the quenched melt. On annealing, the conformation may change when the energy supplied is sufficient to effect flips of the aromatic and ester groups.

X-Ray diffraction simulation

Figures 6 and *7* show the predicted X-ray scatterings on the equator and first layer line for three arrays of 19 chains of 12 monomers after energy minimization. The three starting models had chains with conformation II and conformation I in types A and B packing. The primary equatorial maxima indexed as $hk = 11/20$ and 02 for the two-chain orthorhombic unit cell that are seen in the experimental data are predicted for all three models (*Figure 6*). For the model with chains in conformation I and type B packing we also predict a significant maximum for $hk = 21$, which is not observed experimentally but arises in the calculations because of the obvious differences between the projections of the two chains in the unit cell onto the *ab* plane. This maximum is very weak or non-existent for the other two models,

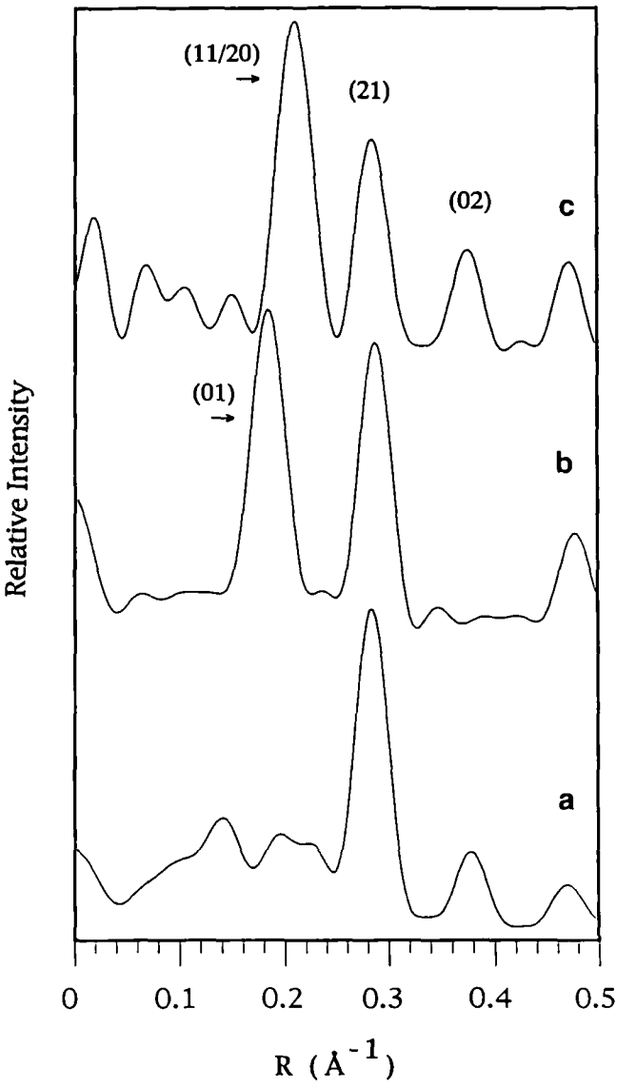

Figure 7 Predicted X-ray scattering on the first layer line for energy-minimized arrays of 19 chains of 12 residues. The starting models had (a) chains with conformation II, (b) type A packing of chains with conformation I and (c) type B packing of chains with conformation I

for which the chains in projection appear more nearly identical. The other peaks are subsidiary maxima because of the small lateral size of the arrays. On the first layer line (*Figure 7*) all three models generate the observed $hk=21$ maximum that is characteristic of three-dimensional order. This is the only observed first layer line maximum predicted by the model containing chains in conformation II. For the models containing chains in conformation I, we also predict maxima indexed as $hk=01$ for type A packing and $hk=11/20$ for type B packing, which are unobserved experimentally. Thus, we can conclude that the Bragg reflections seen on the equator and first layer line are predicted even by these small arrays of 19 chains of 12 monomers in different random sequences. Best agreement is obtained for the model in which the chains have conformation II, i.e. a random orientation of the ester carbonyls consistent with a basic herring-bone packing of the monomers on adjacent chains.

Prior to energy minimization, the above arrays were arranged with their central ester oxygens in register, and after refinement there were small axial shifts from this position with a standard deviation $\sigma=0.2$ Å. This compares to the estimate from the X-ray data of $\sigma=2.0$ Å, based on the distortions necessary to eliminate the Bragg sampling on all but the first layer line[3]. Within the range $\sigma=0.2$–2.0 Å, the main effect on the first layer line is to reduce the intensities, and broadening effects are secondary. Consequently the different σ value does not affect the above conclusions.

Line-broadening measurements for the observed equatorial reflections point to crystallite widths of at least 60 Å, which corresponds to ordered arrays of 150 chains or more. Such models are too large for minimization on our system, but we present here the results of X-ray simulations for unminimized models consisting of 127 tetramers of random sequences arranged with their central ester oxygens in register. Again these are for models containing chains (tetramers) in conformation II and conformation I in types A and B packing. The calculated intensities on the equator and the first layer line are shown in *Figures 8* and *9*. All three models give the $hk=11/20$ and 02 reflections on the equator; for type B packing we also see an $hk=21$ reflection. On the first layer line, all three models generate the observed $hk=21$ peak; for the models of conformation I we also obtain a strong 11 peak for type B packing and a strong 01 peak for type A packing; for the model of conformation II we see a weaker $hk=11$ peak. If the models were to be optimized by energy minimization, it is likely that the weaker peaks would be smoothed away. Thus, the results

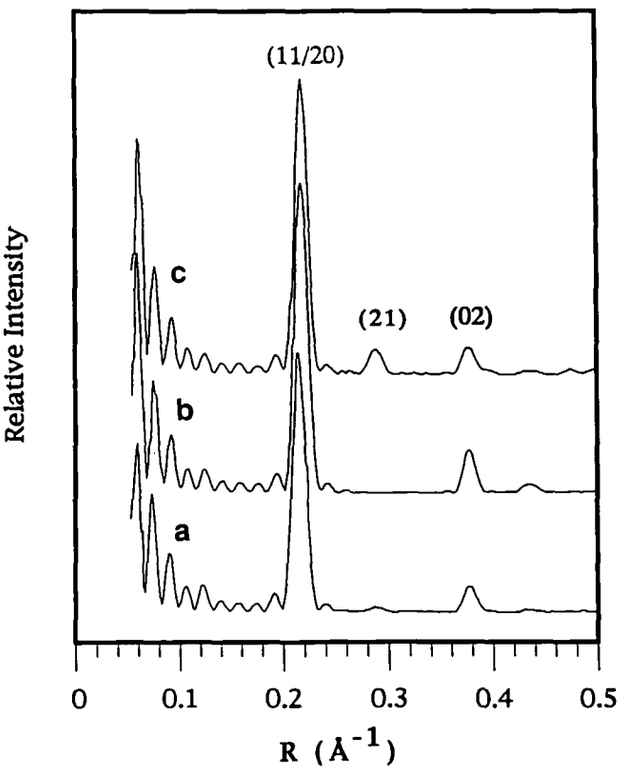

Figure 8 Predicted X-ray scattering on the equator for three un-optimized arrays of 127 tetramers: (a) chains with conformation II; (b) type A packing of chains with conformation I; (c) type B packing of chains with conformation I

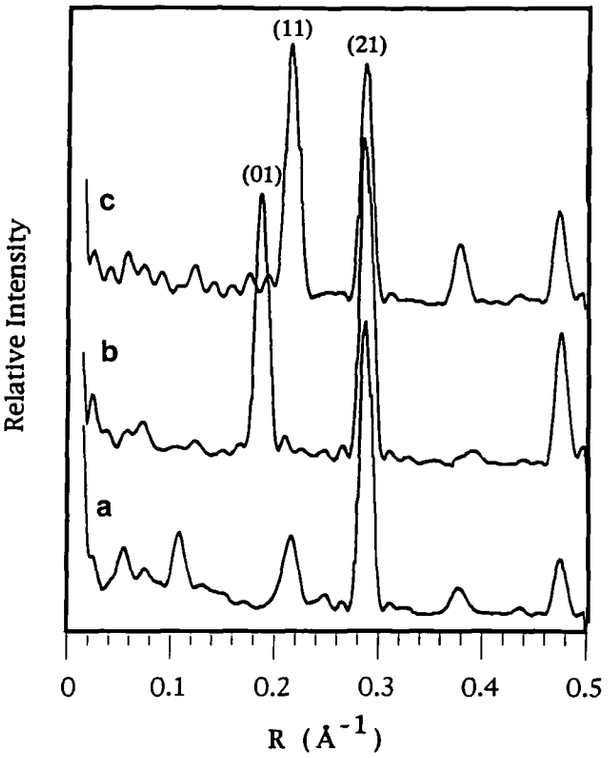

Figure 9 Predicted X-ray scattering on the first layer line for three unoptimized arrays of 127 tetramers: (a) chains with conformation II; (b) type A packing of chains with conformation I; (c) type B packing of chains with conformation I

for the larger unoptimized models parallel those for the smaller optimized arrays, and also show a preference for the structure containing chains in conformation II. These data indicate that we can draw significant structural conclusions from optimizations performed on the relatively small arrays of 19 chains of 12 monomers.

All the arrays of 19 chains reproduce approximately the positions of the main meridional maxima. The deviations are within the range expected when we use a small sample of all the possible sequences. The intensities match reasonably well, except for the first maximum, which is predicted to be much weaker than is observed. Increasing the number of chains in the arrays has the effect of 'concentrating' the layer line intensity in the meridional region, and this effect is most appreciable for the first maximum, with the result that the observed peak is more intense than that calculated. It is interesting that for unoptimized arrays of 19 antiparallel (alternating up and down) chains, the first maximum on the meridian is predicted to be extremely weak and would be essentially unobservable. This intensity is somewhat enhanced for the optimized antiparallel structure, in which the axial registration is less perfect, but it is still very weak compared to that predicted for parallel chains. To some extent this observation argues against a regular, alternating, antiparallel array of chains, and presently we favour random packing of up and down chains.

CONCLUSIONS

The molecular modelling and X-ray simulations favour a structure formed by minimal registration of short chain segments of a completely random HBA/HNA sequence. The segments are packed on the observed pseudo-hexagonal lattice with approximate registration at their centres. Following molecular mechanics energy minimization, the potential energy falls to a value that is very similar to that obtained for an analogous homopolymer model. It appears that there is sufficient free volume in the structure to allow the monomers to adjust their torsional conformations so as to avoid bad contacts between non-identical sequences. There is no necessity to propose segregation of identical non-repeating sequences in order to effect three-dimensional ordering. Simulations of the X-ray patterns show that even small arrays of 19 non-identical chains of 12 monomers are sufficient to predict the main features of the observed diffraction data. The results favour a structure with a fair degree of randomness in the mutual orientations of successive ester groups. This is the type of structure one would expect to obtain on quenching a nematic array of chains, which might then become more ordered on annealing.

REFERENCES

1 Biswas, A. and Blackwell, J. *Macromolecules* 1988, **21**, 3146
2 Biswas, A. and Blackwell, J. *Macromolecules* 1988, **21**, 3152
3 Biswas, A. and Blackwell, J. *Macromolecules* 1988, **21**, 3158
4 Sun, Z., Cheng, H.-M. and Blackwell, J. *Macromolecules* 1991, **24**, 4162
5 Hanna, S. and Windle, A. H. *Polymer* 1988, **29**, 207
6 Golombok, R., Hanna, S. and Windle, A. H. *Mol. Cryst. Liq. Cryst.* 1988, **155**, 281
7 Johnson, D. J., Karacan, I. and Tomka, J. G. *Polymer* 1990, **31**, 8
8 Jung, B. and Schurmann, B. L. *Makromol. Chem., Rapid Commun.* 1989, **10**, 419
9 Jung, B. and Schurmann, B. L. *Macromolecules* 1989, **22**, 477
10 Atkins, E. D. T., Thomas, E. L. and Lenz, R. W. *Mol. Cryst. Liq. Cryst.* 1988, **155**, 263
11 Atkins, E. D. T., Thomas, E. L. and Lenz, R. W. *Mol. Cryst. Liq. Cryst.* 1988, **155**, 271
12 Chin, H. H., Azaroff, A. and Lenz, R. W. *J. Polym. Sci., Polym. Phys. Edn* 1989, **27**, 1993
13 Chin, H. H., Azaroff, A. and Lenz, R. W. *J. Polym. Sci., Polym. Phys. Edn* 1989, **27**, 2001
14 Blackwell, J. and Gutierrez, G. A. *Polymer* 1982, **23**, 671
15 Gutierrez, G. A., Chivers, R. A., Blackwell, J., Stamatoff, J. B. and Yoon, H. *Polymer* 1983, **24**, 937
16 Chivers, R. A., Blackwell, J. and Gutierrez, G. A. *Polymer* 1984, **25**, 435
17 Blackwell, J., Gutierrez, G. A. and Chivers, R. A. *Macromolecules* 1984, **17**, 1219
18 Chivers, R. A. and Blackwell, J. *Polymer* 1985, **26**, 997
19 Troughton, M. J., Unwin, A. P., Davis, G. R. and Ward, I. M. *Polymer* 1988, **29**, 1389
20 Yoon, D. Y., Masciocchi, N., Depero, L. E., Viney, C. and Parrish, W. *Macromolecules* 1990, **23**, 1793
21 Lieser, G. *J. Polym. Sci. Polym. Phys. Edn* 1983, **21**, 1611
22 McCullagh, C. M., Blackwell, J. and Jamieson, A. M. *Macromolecules* 1994, **27**, 2996
23 Iannelli, P., Masciocchi, M., Parrish, W. and Yoon, D. Y. *Bull. Am. Phys. Soc.* 1990, **35**, 1506
24 Sun, Z. and Blackwell, J. unpublished results
25 Adams, J. M. and Morsi, S. E. *Acta Crystallogr. B.* 1976, **32**, 1345
26 Lautenschläger, P., Brickmann, J., van Ruiten, J. and Meier, R. J. *Macromolecules* 1991, **24**, 1284
27 van Ruiten, J., Meier, R. J., Hahn, C., Mosell, T., Sanban, A. and Brickmann, J. *Macromolecules* 1993, **26**, 1555
28 Coulter, P. and Windle, A. H. *Macromolecules* 1989, **22**, 1129
29 Bicerano, J. and Clark, H. A. *Macromolecules* 1988, **21**, 585
30 Hong, S.-K. and Blackwell, J. *Polymer* 1989, **30**, 225
31 Hong, S.-K. and Blackwell, J. *Polymer* 1989, **30**, 780